Pure & Appl. Chem., Vol. 63, No. 10, pp. 1465–1472, 1991.
Printed in Great Britain.

Alternative refrigerant properties measurement and correlation program at NIST (national institute of standards and technology)

Graham Morrison

Thermophysics Division, Center for Chemical Technology
National Institute of Standards and Technology, Gaithersburg, MD. (USA) 20899

Abstract - The activities in the Thermophysics Division at NIST to produce both property measurements and correlations are discussed. These activities are directed toward providing information about materials that will be alternatives to the fully halogenated compounds presently used as working fluids. Seven property measurement apparatuses and three property correlation projects are described.

1. INTRODUCTION

The Thermophysics Division at the United States National Institute of Standards and Technology (NIST, formerly the National Bureau of Standards) has a tradition of measurement, data correlation, and development of new representations for properties of fluids that are important to commerce. There has been a program over the past decade to measure and to represent the properties of refrigerants (ref. 1). Initially, this project was directed toward the study of mixtures as alternative working fluids in domestic heat pumps (ref. 2). More recently, this work has been directed toward measuring, correlating, and predicting the properties of materials to serve as alternatives for the fully halogenated chlorofluoromethanes and ethanes, particularly dichlorodifluoromethane (R12) and trichlorofluoromethane (R11).

In this paper, research in progress will be discussed. In Section 2., seven experiments in the Fluid Sciences Group of the Thermophysics Division will be described. The result of this program is a coherent set of data from which a thermodynamic surface can be generated. In Section 3, three data correlation projects, two in the Division and one supervised by it, will be described.

2. THE EXPERIMENTAL MEASUREMENT PROGRAM

The goals of the program described in this section are several fold: first, to produce a wide-ranging, multiproperty set of data for a fluid; second, to develop new measurement techniques and to refine classical ones; and finally, to produce data of reference state quality. These measurements are made with the following apparatuses:

a. Variable-volume VLE cell.
b. Burnett, gas-phase PVT apparatus.
c. High-pressure, oscillating-tube densimeter.
d. Low and high pressure ebulliometers.
e. Surface tension and refractive index cell.
f. Dielectric constant measurement cell.
g. Spherical acoustical resonator.

a. Variable-volume VLE cell

Measurements with the variable volume VLE cell produces the saturated liquid and vapor densities and the vapor pressure. These data establish a benchmark in the phase diagram around which the other measurements are made. The cell, shown in Fig. 1a, is constructed from a drawn sapphire tube that is closed on the ends with stainless steel plugs and o-rings (ref. 3).

All the measurements are made with the sample in two phases. During the sequence of measurements the total volume is changed so that the relative amounts of liquid and vapor changes; the pressure is measured simultaneously. The extrapolation of the liquid volumes measured at a particular temperature to zero vapor volume leads to the saturated liquid density and vapor pressure. The ratio of the change of the liquid volume as the vapor

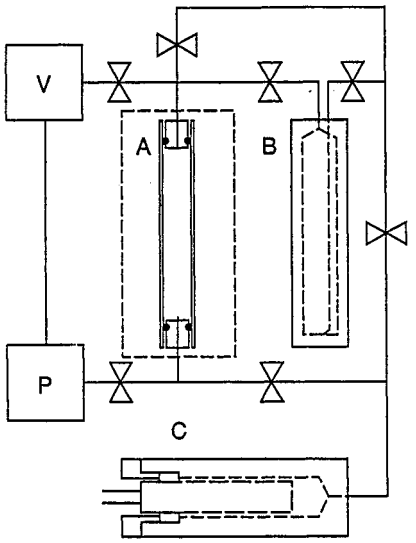

Figure 1a. A schematic diagram of the variable volume VLE cell: A - the cell; B - the sample transfer vessel; C - the volumetric mercury injector; V - vacuum line; P - pressure gauge (ref. 3).

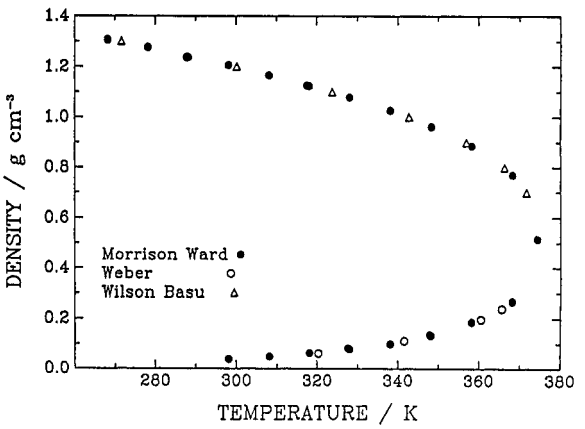

Figure 1b. Saturation boundary for R134a. Morrison/Ward (ref. 3), Weber (ref. 4), Wilson/Basu (Int. Journ. of Thermophysics, 10, 591 (1989).)

volume is changed is the ratio of the vapor density to the liquid density; thus the saturated vapor densities are simultaneously accessible. The accuracy of the liquid density is on the order of 0.3%; the accuracy of the vapor density is on the order of 0.04 g cm^{-3}. The same cell can be used to determine critical point conditions by direct observation of the location of the developing meniscus from the homogeneous fluid as a function of total volume. Critical volumes can be determined to 0.3% and the temperature to 10 mK. Figure 1b shows the saturation boundary for 1,1,1,2-tetrafluoroethane (R134a) determined by this method; other data are shown for comparison (ref. 3).

b. Burnett, gas-phase PVT apparatus

A semiautomated PVT apparatus of the Burnett type has been used to measure the properties of 1,1,1,2-tetrafluoroethane (R134a) and 1,1-dichloro-2,2,2-trifluoroethane (R123) from 40 °C to 180 °C (refs. 4 and 5). This instrument, represented schematically in figure 2, has been thoroughly documented elsewhere (ref. 6). These data consist of at least one set of Burnett expansions. The range of densities is determined by the material. In addition, five different isochores that intersect the Burnett isotherm are measured. The distinguishing feature of this apparatus is the automated pressure balance, which allows the pressure transducer to be nulled automatically when the instrument is run in the isochoric mode. The

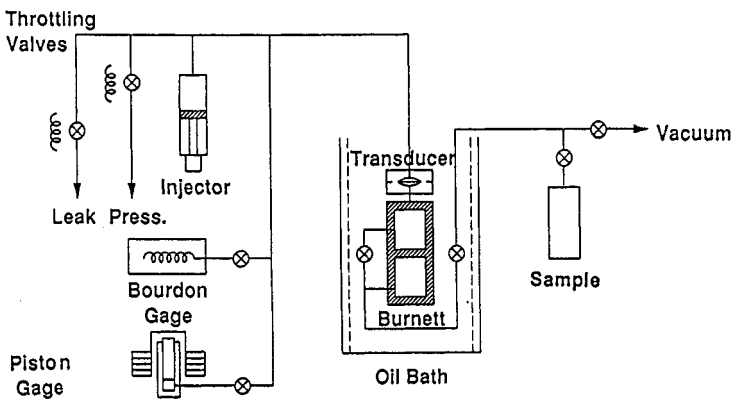

Figure 2. A schematic diagram of the Burnett apparatus (ref. 4).

isochores can be used to determine saturation densities by noting the change in slope of the pressure with respect to temperature. Finally, by filling the apparatus to the critical density and lowering the temperature, one can measure the equilibrium vapor pressure. For all the measurements, the data are recorded in a minicomputer and stored for later processing. Data from this instrument is referred to in Figs. 1b and 5b.

c. High pressure oscillating tube densimeter

The complementary density information to that provided by the VLE and Burnett apparatuses is the compressed liquid density. Densities are measured from - 10 °C to 110 °C and from the saturation pressure to 6500 kPa with a stainless steel vibrating tube densimeter. The cell containing the tube is surrounded by a steel jacket with a water/ethylene glycol mixture circulating through it. The entire apparatus is kept inside an temperature controlled air bath. The temperature of the circulating fluid and the outer surface of the steel jacket are monitored to be certain that the temperature of the tube is known. The temperature is controlled to 0.005 K and is accurate to 0.01 K. The densimeter was calibrated over the entire temperature and pressure range with degassed, distilled water. The Haar et al. (ref. 7) representation of water was used to determine the densities for the calibration. A detailed description of the experimental set-up can be found in reference 3. The apparatus is shown schematically in Fig. 3.

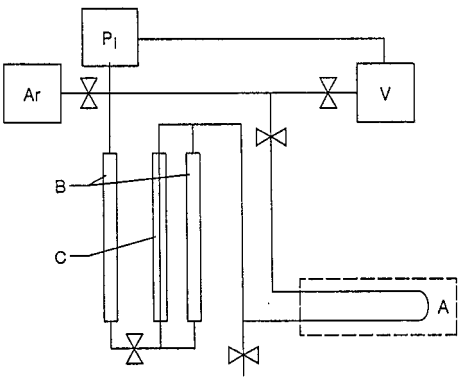

Figure 3. A schematic diagram of the vibrating tube densimeter: A - the vibrating tube in its thermostat; B - the mercury manometer pressure transducer; C - mercury level sight glass; P1 - pressure gauge; V - vacuum line; Ar - argon pressurizing line (ref. 3).

To test the accuracy of the instrument, the density of dichlorodifluoromethane (R22) was measured over the range of the instrument, shown in Fig. 4a., and was compared to the Japanese Association of Refrigeration (JAR) representation of of R22 (ref. 8). Figure 4b shows the comparison to the JAR representation and the isochoric measurements made by Zander

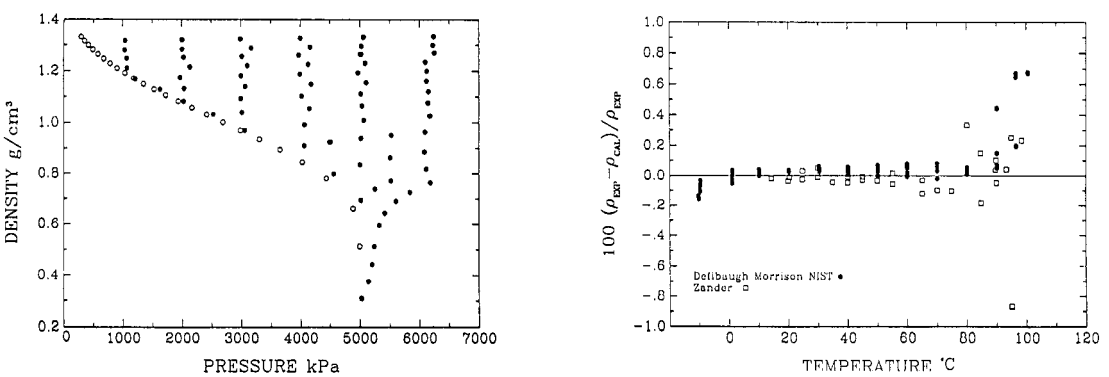

Figure 4a. Pressure density data for R22; b. deviation from the JAR fit to the properties of R22 (ref. 8).

(ref. 9). In the compressed liquid phase below the critical temperature, t = 96.15 ^{0}C, the measurements agree with the surface and the data within the claimed accuracy of the Zander's measurements. Near the critical point, the deviations are as much as 2 % from the JAR surface. We note also, considerable scatter in Zander's measurements. It is likely that the vibration of the tube has a serious effect on the density of the fluid in this region where small uncertainties in the temperature and the pressure become important.

Saturation densities have been determined by measuring density near to but above the vapor pressure, and extrapolating the measurements to the vapor pressure. Figure 5 shows the density of 1,1-dichloro-2,2,2-trifluoroethane (R123) determined in this way (ref. 3), Those data are compared to the following correlation function:

$$\rho_l/g\ cm^{-3} = 0.550 + 0.001157135\ (456.94 - T/K) + 0.158652\ (456.94 - T/K)^{0.300897}$$

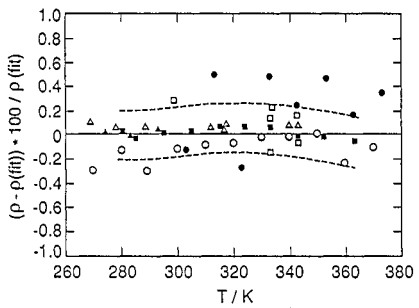

Figure 5. The density of saturated liquid R123: closed circles - VLE cell; closed squares vibrating tube densimeter; closed triangles - ambient pressure buoyancy measurement (ref. 3).

d. Low and high pressure ebulliometers

The apparatuses described in parts a. and b. of this Section are both used to determine vapor pressure. The measurements in the VLE cell and the Burnett apparatus are both static measurements. The ebulliometer utilizes a steady-boiling state to determine vapor pressure. Although this approach has its own uncertainties associated with the equilibrium of the fluid condensing on the temperature sensor, these measurements complement the static measurement.

The low-pressure ebulliometer, shown schematically in figure 6a, is constructed from borosilicate glass; it is a modification of a boiler designed by Ambrose (ref. 10). It consists of two boilers separated by liquid nitrogen traps. One boiler contains the reference fluid, water; the other contains the fluid of interest. The entire system is pressurized with helium. The liquids in the boilers are warmed to effect steady boiling in both. The vapor condenses on the glass well holding a long-stem 25 Ω platinum resistance thermometer extending down the center of the reflux condensor above the boiler. The pressure in the system is determined by knowing the condensation temperature of the reference fluid. The pressure range, limited by the strength of the glass system, is from 0 to 150 kPa.

The boiler of high-pressure ebulliometer is constructed from a sapphire tube with end plugs similar to those of the VLE cell. The remainder of the apparatus is constructed from stainless steel, the apparatus is shown schematically in Fig. 6b. A dry-ice/acetone trap is located between the boiler and the pressure sensor to stop migration of material from the boiler into the pressure sensor. The system is pressurized with helium. The condensation temperature is measured with a 100 Ω platinum resistance thermometer in a stainless steel sheath that extends down the middle of the reflux condensor. This apparatus has been used between 0 and 2.5 x 10^{3} kPa; however, it can be used up to 1 x 10^{4} kPa.

Figure 7 shows vapor pressure measurements for 1,1-dichloro-2,2,2-trifluoro- ethane (R123) made using the VLE cell, the Burnett apparatus, and the two ebulliometers compared to the following correlation of Weber (ref. 11):

$$\ln(p/kPa) = -9.0615600 / T_r + 20.864032 - 4.517520\ T_r + 0.9233036\ T_r^3 + 1.114003\ (1 - T_r)^{1.5}$$

where $T_r = T / 456.94$ K

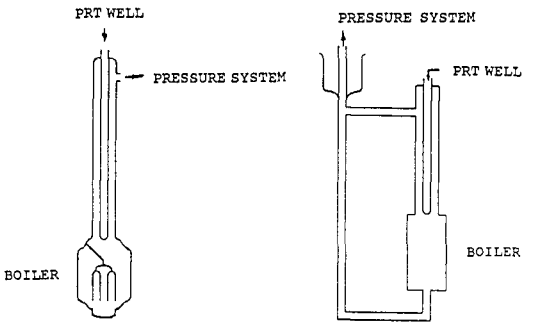

Figure 6a. Schematic of the low pressure, comparitive ebulliometer; b. the high pressure ebulliometer.

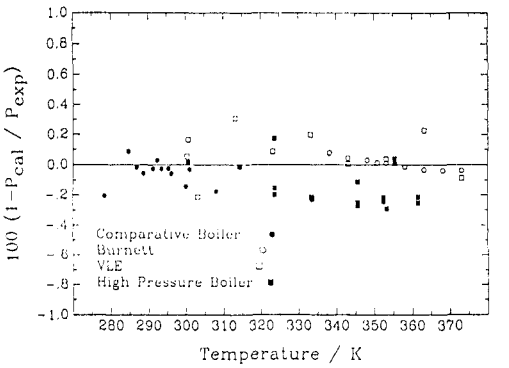

Figure 7. Comparison of four sets of vapor pressure measurements for R123:

e. Refractive index and surface tension

Although the surface tension is not a quantity needed to produce a thermodynamic surface, it is an important for correlating the heat transfer coefficient in the nucleate regime multiphase boiling (ref. 12). The measurement is made in a pill-box shaped sapphire and steel cell that contains four capillaries of different diameter and a prism. The details of the measurement are described by Chae et al. (ref. 13). The prism is used to measure the deflection of laser beams (He-Ne) that pass through the liquid and the vapor phases. The deflection measurement yields the refractive index and, through the Lorentz-Lorenz relation, the density of the liquid and vapor phases. This transformation requires that the liquid density at one set of saturation conditions be known and that the molecular polarizability is independent of density. Extensive measurements on water (ref. 14), both liquid and vapor, show this assumption to be accurate to within 2%. over a huge range of conditions.

The densities of the coexistent liquid and vapor phases lead both to the evaluation of the surface tension and to the critical point temperature and density. Those fluids with critical points above 380 K have been determined in this way. Chae et al. have reported properties for a number of altenative refrigerants (ref. 15).

f. Dielectric constant cell

The dielectric properties of refrigerants are important for machinery design, particularly for refrigerators and domestic heat pumps where the compressors are hermetically sealed units. In these applications, the refrigerant is in direct contact with the motor windings where it experiences high electric fields. Through the Clausius-Mosotti relation and the Debye relation, the value of the dielectric constant as it depends upon density and temperature can be used to determine two fundamental molecular quantities, the permanent dipole moment and the molecular polarizability. The dielectric constant of nine refrigerants were measured as dilute gases from 305 K to 415 K. The pressure was measured with a quartz pressure transducer. The measurements were made in the capacitance cell used by Greer et al. to measure the rate of recombination of photodissociated chlorine near the critical point (ref. 16). The cell had a vacuum capacitance of about 1 pF and a total volume of roughly 7.0 cm^3. The capacitances were measured to a resolution of 3 ppm. The cell was placed in a temperature controlled oven held constant to 0.2 K. The temperature was measured with a digital output platinum resistance thermometer and was accurate to 10 mK.

The first seven of the nine refrigerants reported in Table 1. (ref. 17) have temperature independent dipole moments. Although these molecules can undergo internal rotation, the conformers are degenerate. The last two have confomers that are not degenerate, having distinct trans and gauche forms with different dipole moments, whose relative populations vary with temperature. Although all the information necessary for separating the contribution of the conformers is available from the dielectric constant information, those measurements were supplemented with refractive index and density measurements of the liquid and infra-red spectral measurements when that was available from the literature.

Table 1. Dipole moments and molecular polarizabilities of nine refrigerants (the precision is noted parenthetically)

Material			μ / Debye	α / $cm^3 mol^{-1}$
pentafluoroethane (R125)			1.561(0.006)	14.3(0.3)
1,1,1,2-tetrafluoroethane (R134a)			2.060(0.010)	13.8(0.7)
1,1,1-trifluoroethane (R143a)			2.333(0.008)	14.4(0.6)
1,1-difluoroethane (R32)			2.270(0.007)	13.2(0.5)
1-chloro-1,2,2,2-tetrafluoroethane (R124)			1.460(0.011)	18.4(0.5)
1,1-dichloro-2,2,2-trifluoroethane (R123)			1.59(0.07 - preliminary value)	
1,1-dichloro-1-fluoroethane (R141b)			2.09(0.07 - preliminary value)	
1,1,2,2-tetrafluoroethane (R134)		(trans)	0.0	13.9(0.7)**
		(gauche)	2.44(0.04)	
1,1,2-trifluoroethane	(R143)	(trans)	1.58(0.05)	13.9(0.7)**
		(gauche)	3.00(0.12)	

** estimated

g. Spherical acoustical resonator

The measurements described thus far provide information to produce a p-V-T equation of state. One requires the ideal gas heat capacity to produce the complete thermodynamic surface. Measurement of the speed of sound, u, extrapolated to zero pressure leads to this information through the following relationship:

$$u^2 = \gamma_o RT/M \quad \text{where M is the molar mass,}$$

$$\gamma_o = C_p^o / C_v^o \quad \text{and} \quad C_p^o = \gamma_o R / (\gamma_o - 1)$$

The resonator is a spherical shell with an internal volume of about 1/8 liter shown in schematic form in figure 8 (ref. 18). The spherical geometry has several advantages over other geometries: the low surface to volume ratio of the sphere leads to a lower dissipation in the thermal boundary layer than for other geometries; the measurements utilize low-order, radially symmetric modes, which are non-degenerate and have resonance frequencies that are insensitive to geometric imperfection in the cavity; finally, the measurements are not subject to viscous dissipation at the walls, which contributes significantly to the high precision with which the resonance frequencies can be determined. This apparatus is designed to operate from 230 K to 340 K and at pressures up to 575 kPa.

This instrument has been used to determine the ideal gas heat capacity of R134a and R123. Ideal gas heat capacity is nominally accessible from spectroscopic data; however, as the molecules become larger, accurate determination of all the energies associated with the internal modes becomes more difficult; the greatest uncertainty is often in those modes that contribute the most to the heat capacity.

Measurement of the speed of sound is an alternative way to measure other gas properties, in particular the virial coefficients. The square of the speed of sound can be written as a virial expansion in a manner similar to the compressibility factor as follows:

$$u^2 = (RT\gamma_o/M)[1 + (\beta_a/RT)p + (\gamma_a/RT)p^2 + \ldots$$

where β_a and γ_a are the second and third acoustic virial coefficients, respectively. These quantities are directly connected to the ordinary virial coefficients. Figure 9 shows the excellent agreement between the two determinations of the second virial coefficient. The third virial coefficients agree less well. The difference may be, in part, due to inadequacies in the square-well model used to reconcile the two measurements (ref. 19).

The value of the heat capacity plays a subtle, but important role in machinery design. Figure 10a shows a schematic refrigeration cycle in a temperature-entropy diagram. The value of the heat capacity is intimately connected to the shape of the two-phase region through the following relationship:

$$dT/dS(sat) = [C_v / T + (\partial p/\partial T)_v \, dv/dT(sat)]^{-1}$$

The value of heat capacity becomes progressively larger as the molecules become more complex; indeed, it is possible for the vapor side of the two-phase region to have a re-entrant portion as shown in Fig. 10b. In such a circumstance, the thermodynamic path of the fluid in the compressor could lead it into the two-phase region. The formation of a liquid in the compressor can, over the long run, cause serious damage.

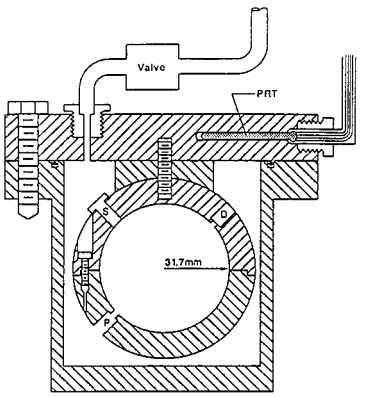

Figure 8. Cross sectional representation of the spherical acoustic resonator (ref. 18).

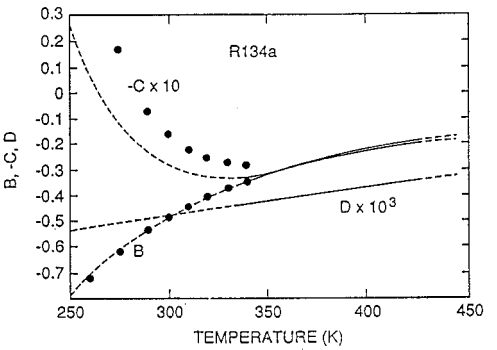

Figure 9. Virial coefficients from the Burnett measurement (solid lines) and resonator (closed circles). Dashed lines are extension of the Burnett determinations.

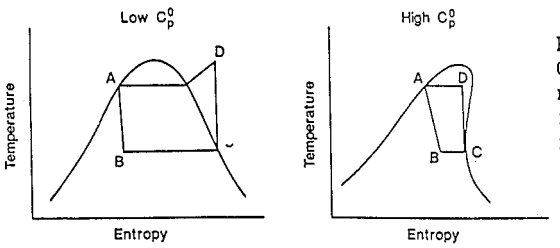

Figure 10a. Temperature-entropy diagram when Cv is small and b., Cv is high. ABCD represents a refrigeration cycle: AB, isenthalpic expansion; BC, evaporation; CD, isentropic compression; DA, condensation.

3. DATA CORRELATION

In this Section, three data correlation schemes will be discussed. The first is based on a simple model, a perturbation of the Carnahan-Starling representation of the hard-sphere fluid. The second and third schemes are based on functions that have large numbers of parameters.

The simplest of these correlations is based upon a modified hard-sphere equation of state described in detail in references 1 and 20. Because De Santis et al. (ref. 20) were among the first to use this function to describe mixtures, it has been called the Carnahan - Starling - DeSantis (CSD) equation of state. It has been used at NIST to correlate the properties of refrigerant mixtures in applications where the equation of state would be called up to 10^5 times. The thermodynamic function routines have recently been packaged as OSRD (NIST Office of Standard Reference Data) database no. 23, known as REFPROP (ref. 21) In this function, the parameters "a" and "b" are allowed to have a temperature dependence leading to six coefficients. These six parameters are typically determined from saturation data alone; Morrison and McLinden (ref. 22) have shown that in situations where there are more extensive sets of data, the equation arising from the saturation boundary is nearly optimal. Mixtures are treated with this equation of state by using the Lorentz-Berthelot rules to determine "a" and "b" for the mixtures. The departure of the value of "a" from the geometric mean of the pure component values for the unlike interaction is treated with a correction term, (1 - f_{12}). The library now contains data for 24 binary mixtures. REFPROP can perform calculations for mixtures with as many as five components.

A second correlation scheme for refrigerants that is being developed in the Thermophysics Division (ref. 23) is based on the extension of corresponding states developed by Leland and Chappelear (ref. 24). This program, an extension of the SuperTRAPP routines, is based upon a 32 parameter modification of the Benedict - Webb - Rubin equation of state described in detail in references 23 and 25. The parameters in this equation of state are based upon the properties of a thoroughly studied material. For the family of refrigerants, 1,1,1,2-tetrafluoroethane, for which pVT, speed of sound, and isochoric heat capacity data now exist from low pressure gas state to compressed liquid states up to 50 MPa and from the triple point to slightly supercritical temperatures, depending upon the property, has been chosen as the reference fluid. A preliminary equation of state for R134a has recently been published (ref. 25). Once the reference equation has been established, the properties of

any other fluid can be predicted by the appropriate transformation operation. This approach has the advantages that little information about another material is required once the reference function is known and, to the extent that the model is physically valid, the properties of a material can be estimated accurately. The disadvantages lie in the complexity of the algorithm for the user who needs to call a routine often.

The final correlation program, being carried out at the Center for Applied Thermodynamic Studies, University of Idaho, is supported in part by the NIST Standard Reference Data Program in close cooperation with the Thermophysics Division. The equation of state begins with a 90 term equation of the Benedict - Webb - Rubin type. Only a fraction of these terms are retained by using a least squares selection algorithm originally developed by Wagner (ref. 26), adapted for equations of state by de Reuck and Armstrong (ref. 27) and further modified by Bjorn (ref. 28).

Acknowledgements

The author wishes particularly to thank Mr. Dana R. Defibaugh, Dr. Christopher W. Meyer, Dr. James W. Schmidt, and Dr. Lloyd A. Weber for their assistance in assembling this manuscript. This work has been supported in part by the United States Department of Energy, the Office of Standard Reference Data of NIST, the Electric Power Research Institute, and the American Society of Heating, Refrigerating and Air-Conditioning Engineers. Samples of materials have been donated by Allied-Signal Corporation, E.I. DuPont de Nemours Co., and Atochem North America (formerly Pennwalt) Corp.

REFERENCES

1. G. Morrison and M.O. McLinden, "Application of a Hard Sphere Equation of State to Refrigerants and Refrigerant Mixtures," NBS Technical Note 1226, U.S. Department of Commerce, Washington (1986).
2. J.A. Calm and D.A. Didion, ASHRAE Technical Data Bulletin, "Advances in Nonazeotropic Mixture Refrigerants for Heat Pumps," 1, 132-137 (1985).
3. G. Morrison and D.K. Ward, J. Fluid Phase Equilibria, (in press, 1990).
4. L.A. Weber, International Journal of Thermophysics, 10, 617-627 (1989).
5. L.A. Weber, J. Chem. Eng. Data, (in press, 1990).
6. D. Linsky, J.M.H. Levelt Sengers, and H.A. Davis, Rev. Sci. Instrum., 58, 817 (1987).
7. L. Haar, J.S. Gallagher, and G.S. Kell, NBS/NRC Steam Tables, Hemisphere Publishing, New York (1984).
8. Japanese Association of Refrigeration (JAR), Thermophysical Properties of Refrigerants, Chlorodifluoromethane (R22), Tokyo (1975).
9. M. Zander, Proc. 4th Symp. on Thermophys. Prop. of Gases, Liq., and Solids, ASME, 114 (1968).
10. D. Ambrose, J. Sci. Inst, 1, 41 (1968).
11. L.A. Weber, Proceedings of the 1990 USNC/IIR-Purdue Refrigeration Conference, (in press, 1990).
12. D. Butterworth and G.F. Hewitt, Two-Phase Flow and Heat Transfer, 138-141, Oxford University Press (1984).
13. H.B. Chae, J.W. Schmidt and M.R. Moldover, J. Chem. Eng. Data, 35, 6-8, (1990).
14. P. Schiebener, J. Straub, J.M.H. Levelt Sengers and J.S. Gallagher, J. Phys. Chem. Ref. Data (in press, 1990).
15. H.B. Chae, J.W. Schmidt, and M.R. Moldover, J. Phys. Chem., (in press, 1990).
16. S.C. Greer, Phys. Rev. A31, 3240 (1985).
17. C.W. Meyer and G.Morrison, J. Phys. Chem., (submitted for publication, 1990).
18. A.R.H. Goodwin and M.R. Moldover, J. Chem. Phys., (in press, 1990).
19. C.M. Knobler, Chemical Thermodynamics, vol. 2, M.L. McGlashan, ed., 199-237, The Chemical Society, London (1978).
20. R. DeSantis, F. Gironi, and L. Marrelli, Ind. Eng. Chem., Fundam., 15, 183 (1976).
21. National Institute of Standards and Technology, Office of Standard Reference Data, Database no. 23, Gaithersburg, MD (1989).
22. G. Morrison and M.O. McLinden, ASME Paper 86-WA/HT-59, (1986).
23. J.F. Ely, Proceedings of the 1990 USNC/IIR-Purdue Refrigeration Conference, 383-392 (1990).
24. T.W. Leland and P.S. Chappelear, Ind. Eng. Chem, 60, 15-43 (1968).
25. M.O. McLinden, J.S. Gallagher, L.A. Weber, G. Morrison, D. Ward, A.R.H. Goodwin, M.R. Moldover, J.W. Schmidt, H.B. Chae, T.J. Bruno, J.F. Ely, and M.L. Huber, ASHRAE Transactions 95, 263 (1989).
26. W. Wagner, Berichte der VDI Zeitschriften, 3, 39 (1974).
27. K.M. deReuck and B. Armstrong, Cryogenics, 19, 505-512 (1979).
28. K.R. Bjorn, "Linear Least-Squares Regression Algorithm for the Optimization of Thermodynamic Equations of State, Thesis, University of Idaho, Moscow, ID (1988).
29. R.B. Stewart, R.T. Jacobsen, and S.G. Penoncello, "Thermodynamic Properties of Refrigerants," ASHRAE (1986).